Theory of Time-Resolved Sum-Frequency Generation and Its Applications to Vibrational Dynamics of Water

Michitoshi Hayashi,*,†,‡ Ying-Jen Shiu,§ Kuo Kan Liang,∥ Sheng Hsien Lin,⊥ and Yuan Ron Shen#

Center for Condensed Matter Sciences, National Taiwan University, Taipei 106, Taiwan, Institute for Molecular Sciences, Okazaki, 444-8585, Japan, Institute of Atomic and Molecular Sciences, Academia Sinica, Taipei 106, Taiwan, Research Center for Applied Sciences, Academia Sinica, Taipei 115, Taiwan, Department of Applied Chemistry, National Chaio-Tung University, Hsin-Chu 300, Taiwan, and Department of Physics, University of California, Berkeley, California 94720

A molecular theory of time-resolved sum-frequency generation (SFG) has been developed. The theoretical framework is constructed using the coupled-oscillator model in the adiabatic approximation. This theory can treat not only the vibrational spectroscopy but also vibrational dynamics. An application of this theory is also provided for estimation of the time constants of the intermolecular vibrational energy transfer between water molecules. This approach can be used for molecular analysis of the experimental results of Shen at al. on the SFG studies of vibrational dynamics of water.

1. Introduction

Molecular theory for various kinds of sum-frequency generation (SFG) has been developed. However, few theoretical treatments for time-resolved SFG have been reported. Recently, Shen et al.[1] have reported the femtosecond time-resolved vibrational IR-UV SFG for studying the vibrational dynamics of water surface molecules. In this paper, we shall report a molecular theory of femtosecond time-resolved IR-UV SFG.

Although numerous MD calculations have been performed to study the vibrational spectroscopy and dynamics of water,[2–6] it still seems desirable to develop a theoretical model that can be used to analyze the experimental data of spectroscopy and dynamics of water. For this purpose, in this paper we divide the whole water system into the vibron (intramolecular vibrations) system and the phonon (librations and intermolecular vibrations) bath. The interactions among different vibrational modes are described by anharmonic couplings and the adiabatic approximation is introduced as a basis set. In vibrational spectroscopy, we show how to calculate the spectral shift, intensity of phonon-side bands, temperature effect, and vibration band-shape functions. In vibrational dynamics, we show how to calculate the vibrational excitation energy transfer between different water molecules and the vibrational relaxation due to one-vibron processes, two-vibron processes, and three-vibronic processes.

The present paper is organized as follows. In section 2 we briefly present the molecular theory of time-resolved SFG, which will be followed by the description of a coupled oscillator model applied to vibrational spectroscopy and vibrational dynamics (section 3). The applications of the theory to estimate the time constants for the intermolecular energy transfer are given in section 4.

* Corresponding author. E-mail: atmyh@ntu.edu.tw.
† National Taiwan University.
‡ Institute for Molecular Sciences.
§ Institute of Atomic and Molecular Sciences, Academia Sinica.
∥ Research Center for Applied Sciences, Academia Sinica.
⊥ National Chaio-Tung University.
University of California.

2. General Theory

Let us consider a model for the pump–probe vibrational IR-UV sum-frequency generation experiments in which an IR-pump laser beam is applied to a sample and, with time delay Δt, other IR and UV laser beams are sent to the sample to generate IR-UV SFG. In this case, we start with[7–10]

$$I(\Delta t) \sim \langle |\hat{e}_{\text{SFG}} \cdot \vec{P}_{\text{pump}}^{\text{SFG}}(\Delta t)|^2 \rangle \qquad (2\text{-}1)$$

where $\vec{P}_{\text{pump}}^{\text{SFG}}(\Delta t)$ represents the nonlinear polarization vector due to the probing lasers in the presence of the pump laser, $\langle \cdots \rangle$ denotes the average over the heat-bath modes and orientation configurations of the molecules, and $\hat{e}_{\text{SFG}}$ represents the polarization unit vector for the vibrational IR-UV SFG signal detection. On the basis of density matrix method,[11] the nonlinear polarizability for pump–probe vibrational IR-UV can be expressed as

$$\vec{P}_{\text{pump}}^{\text{SFG}}(\Delta t) = \sum_l \vec{P}_{\text{pump}}^{\text{SFG}}(l, \Delta t) e^{i\Delta \vec{k} \cdot \vec{R}_l} \qquad (2\text{-}2)$$

where $\vec{P}_{\text{pump}}^{\text{SFG}}(l, \Delta t)$ stands for the nonlinear polarization vector on the molecule at the position $\vec{R}_l$ and $\Delta \vec{k} = \vec{k}_s - \vec{k}_1 - \vec{k}_2$. Substituting eq 2-2 into eq 2-1 and ignoring the incoherent scattering, that is, $l = l'$, yield

$$I(\Delta t) \propto \sum_{l \neq l'} \langle \{\hat{e}_{\text{SFG}} \cdot \vec{P}_{\text{pump}}^{\text{SFG}}(l', \Delta t)\}^* \{\hat{e}_{\text{SFG}} \cdot \vec{P}_{\text{pump}}^{\text{SFG}}(l, \Delta t)\} e^{i\Delta \vec{k} \cdot \vec{R}_{ll'}} \rangle \quad (2\text{-}3)$$

where

$$\vec{P}_{\text{pump}}^{\text{SFG}}(l, \Delta t) = \text{Tr}[(\hat{e}_{\text{SFG}} \cdot \vec{\mu})\hat{\sigma}^{(4)}(t)] = \sum_{nn'} (\hat{e}_{\text{SFG}} \cdot \vec{\mu}_{nn'})\hat{\sigma}_{n'n}^{(4)}(t)$$

$$= (-i)^4 \int_{t_i}^t d\tau_1 \int_{t_i}^{\tau_1} d\tau_2 \int_{t_i}^{\tau_2} d\tau_3 \int_{t_i}^{\tau_3} d\tau_4 \times$$

$$\sum_{nn'} (\hat{e}_{\text{SFG}} \cdot \vec{\mu}_{nn'}) \langle\langle n'n | \tilde{L}'(\tau_1) \, \tilde{L}'(\tau_2) \, \tilde{L}'(\tau_4) \, \tilde{L}'(\tau_3) | \hat{\sigma}(t_i) \rangle\rangle \quad (2\text{-}4)$$

Time-Resolved SFG of Vibrational Dynamics of Water

J. Phys. Chem. A, Vol. 111, No. 37, 2007 **9063**

where $\vec{\mu}$ denotes the electric dipole moment operator, $\hat{\sigma}^{(4)}(t)$ describes the fourth-order reduced density operator with respect to the interaction between radiation field and the molecules, and $\hat{\sigma}(t_i)$ is the initial condition for the reduced density operator. Here $\tilde{L}'(\tau_1)$ is the so-called Liouvillian operator in the interaction representation and $\langle\langle n'n| \cdots |\hat{\sigma}(t_i)\rangle\rangle$ denotes the double-index Liouville space matrix element.

At the phase matching direction, only the molecular pair in the bracket in eq 2-3 at a large distance can contribute to SFG signals. In this case, we find

$$I(\Delta t) \sim$$
$$\sum_{l\neq l'}^{l\,\mathrm{arg}\,e}\langle\{\hat{e}_{\mathrm{SFG}}\cdot\vec{P}_{\mathrm{pump}}^{\mathrm{SFG}}(l',\Delta t)\}^*\rangle\langle\{\hat{e}_{\mathrm{SFG}}\cdot\vec{P}_{\mathrm{pump}}^{\mathrm{SFG}}(l,\Delta t)\}\rangle e^{i\Delta\vec{k}\cdot\vec{R}_{ll'}} \quad (2\text{-}5)$$

To grasp the essence, we assume that the IR pump-pulse and SFG pulses can be approximated by rectangular pulses with the respective pulse durations T_{pump} and T_{SFG}. In the rectangular pulse approximation, the integrals can be divided into two time ranges in eq 2-4 if no overlap between the SFG pulses and pumping pulse is assumed and they are separated by Δt. In this case, we find (see Appendices S1 and S2 in Supporting Information)

$$\langle\{\hat{e}_{\mathrm{SFG}}\cdot\vec{P}_{\mathrm{pump}}^{\mathrm{SFG}}(l,\Delta t)\}\rangle = \sum_{nn'}(\hat{e}_{\mathrm{SFG}}\cdot\vec{\mu}_{nn'}) \times$$
$$\sum_{mm'}(-\mathrm{i})^2\int_0^{T_{\mathrm{SFG}}}d\tau_1\int_0^{\tau_1}d\tau_2\langle\langle n'n|\tilde{L}'(\tau_1+\Delta)\,\tilde{L}'(\tau_2+\Delta)|mm'\rangle\rangle \times$$
$$(-\mathrm{i})^2\int_0^{T_{\mathrm{pump}}}d\tau_3\int_0^{\tau_3}d\tau_4\langle\langle mm'|\tilde{L}'(\tau_3)\,\tilde{L}'(\tau_4)|\hat{\sigma}(t_i)\rangle\rangle \quad (2\text{-}6)$$

where $\Delta = T_{\mathrm{pump}} + \Delta t$ and $\hat{\sigma}(t_i) = \sum_g P(g)|gg\rangle\rangle$, with $P(g)$ being the Boltzmann distribution function. In eq 2-6 the time integrals over τ_1 and τ_2 lead to SFG responses and those over τ_3 and τ_4 give the density matrix for the pumping prepared states. We assume that the IR pumping process with a 130 fs laser pulse cannot generate coherences between vibrationally excited states of any high-frequency vibrational mode at 2800–3800 cm^{-1}. In other words, the pumping process generates populations in the vibrationally excited state g′ or in the vibrationally ground state g. In this case, we find

$$\langle\{\hat{e}_{\mathrm{SFG}}\cdot\vec{P}_{\mathrm{pump}}^{\mathrm{SFG}}(l,\Delta t)\}\rangle = S_{11} + S_{12} + S_{21} + S_{22} \quad (2\text{-}7)$$

where, for example,

$$S_{11} = \sum_e(\hat{e}_{\mathrm{SFG}}\cdot\vec{\mu}_{\mathrm{eg}})\sigma_{\mathrm{eg}\leftarrow\mathrm{gg}}^{\mathrm{SFG}}(T_{\mathrm{SFG}})\,\rho_{\mathrm{gg}}(\Delta t)\,F_{\mathrm{gg}}(T_{\mathrm{pump}})$$
$$(2\text{-}8)$$

and

$$S_{21} = \sum_e(\hat{e}_{\mathrm{SFG}}\cdot\vec{\mu}_{\mathrm{eg}'})\sigma_{\mathrm{eg}'\leftarrow\mathrm{g}'\mathrm{g}'}^{\mathrm{SFG}}(T_{\mathrm{SFG}})\,\rho_{\mathrm{g}'\mathrm{g}'}(\Delta t)\,F_{\mathrm{g}'\mathrm{g}'}(T_{\mathrm{pump}})$$
$$(2\text{-}9)$$

Here $\rho_{\mathrm{gg}}(\Delta t)$ and $\rho_{\mathrm{g}'\mathrm{g}'}(\Delta t)$ denote the time development of the population in the vibrational ground state g and that in the vibrational ground state g′, respectively, and $F_{\mathrm{gg}}(T_{\mathrm{pump}})$ is associated with the pumping condition (see Appendix S3 in the Supporting Information). $\sigma_{\mathrm{eg}\leftarrow\mathrm{gg}}^{\mathrm{SFG}}(T_{\mathrm{SFG}})$ in eq 2-8, for example, can be approximately given by (see Appendices S4, S5, and

S6 in the Supporting Information)

$$\sigma_{\mathrm{eg}\leftarrow\mathrm{gg}}^{\mathrm{SFG}}(T_{\mathrm{SFG}}) = (-\mathrm{i}/\hbar)^2\sum_{g''}(\vec{\mu}_{\mathrm{eg}''}\cdot\vec{E}_{\mathrm{UV}})(\vec{\mu}_{\mathrm{g}''\mathrm{g}}\cdot\vec{E}_{\mathrm{IR}}) \times$$
$$\frac{1}{\mathrm{i}(\omega'_{\mathrm{g}''\mathrm{g}} - \omega_{\mathrm{IR}})}\frac{1}{\mathrm{i}(\omega'_{\mathrm{eg}} - \omega_{\mathrm{IR}} - \omega_{\mathrm{UV}})} \quad (2\text{-}10)$$

The terms S_{12} and S_{22} in eq 2-7 are given in Appendix S5 in the Supporting Information.

In this section, we have derived the time-resolved SFG for studying the population dynamics of surface species. In this paper, we are mainly concerned with the time-resolved IR-UV SFG applied to studying the vibrational energy relaxation (VER) of surface water. In this case, ρ_{gg} (or $\rho_{\mathrm{g}'\mathrm{g}'}$) in eqs 2-8 and 2-9 describes the time-dependent population of vibrational levels. In the next section, we propose a model for vibrational energy transfer, VER, and vibrational spectroscopy for liquid water. Using the Born–Oppenheimer approximation, the vibrational IR-UV SFG has been well treated (see refs 7–10).

3. Coupled Oscillator Model

Liquid water can usually be regarded as consisting of ice-like structures (or clusters) and liquid-like structure (or clusters) which have, in addition to the bending band, 1640 cm^{-1} and the $\nu_{\mathrm{O-H}}$ vibrational band of 3200 cm^{-1}, respectively. For this liquid–vapor interface, there exists the additional dangling-bond structures (or clusters) that have a vibrational band around 3700 cm^{-1}.[1,12,13] To treat the vibrational spectroscopy and dynamics of water, we shall employ the coupled oscillator model; this is reasonable because in the above-mentioned structures (or clusters) the hydrogen-bonding network is formed between water molecules, and the motion between cluster is slow compared with the vibrational dynamics under consideration.

We consider a total system consisting of vibrons (intramolecular vibrational modes) and phonons (external low-frequency modes including librations). The Hamiltonian of the total system can be expressed as

$$\hat{H} = \hat{H}_{\mathrm{s}} + \hat{H}_{\mathrm{b}} + \hat{H}' \quad (3\text{-}1)$$

where $\hat{H}_{\mathrm{s}}$ and $\hat{H}_{\mathrm{b}}$ denote the Hamiltonian for the vibron system and the heat bath, respectively

$$\hat{H}_{\mathrm{s}} = \sum_l\left(\frac{1}{2}\hat{P}_l^2 + \frac{1}{2}\omega_l^2\hat{Q}_l^2\right) \quad (3\text{-}2)$$

$$\hat{H}_{\mathrm{b}} = \sum_j\left(\frac{1}{2}\hat{p}_j^2 + \frac{1}{2}\omega_j^2\hat{q}_j^2\right) = \hat{T}_q + \frac{1}{2}\sum_j\omega_j^2\hat{q}_j^2 \quad (3\text{-}3)$$

and $\hat{H}'$ is the interaction between the system and the heat bath. For $\hat{H}'$ we shall use the anharmonic

$$\hat{H}' = \frac{1}{3!}\sum_l\sum_{j,k}\left(\frac{\partial^3 V}{\partial Q_l\partial q_j\partial q_k}\right)_0 Q_l q_j q_k + \frac{1}{3!} \times$$
$$\sum_{l,l'}\sum_j\left(\frac{\partial^3 V}{\partial Q_l\partial Q_{l'}\partial q_j}\right)_0 Q_l Q_{l'} q_j + \frac{1}{3!}\sum_{l,l',l''}\left(\frac{\partial^3 V}{\partial Q_l\partial Q_{l'}\partial Q_{l''}}\right)_0 Q_l Q_{l'} Q_{l''} +$$
$$\frac{1}{4!}\sum_l\sum_{i,j,k}\left(\frac{\partial^4 V}{\partial Q_l\partial q_i\partial q_j\partial q_k}\right)_0 Q_l q_i q_j q_k + \frac{1}{4!} \times$$
$$\sum_{ll'}\sum_{j,k}\left(\frac{\partial^4 V}{\partial Q_l\partial Q_{l'}\partial q_j\partial q_k}\right)_0 Q_l Q_{l'} q_j q_k + \cdots \quad (3\text{-}4)$$

9064 *J. Phys. Chem. A, Vol. 111, No. 37, 2007*

Hayashi et al.

We shall show that different terms in eq 3-4 play different roles in vibrational spectroscopy and dynamics.

For basis sets, we shall employ the adiabatic approximation,[14] i.e.,

$$\hat{H}\psi_{nv}(Q,q) = E_{nv}\psi_{nv}(Q,q) \tag{3-5}$$

$$\psi_{nv}(Q,q) = \Phi_n(Q,q)\,\Theta_{nv}(q) \tag{3-6}$$

$$\left(\hat{H}_s + \frac{1}{2}\sum_j \omega_j^2 q_j^2 + \hat{H}'\right)\Phi_n(Q,q) = U_n(q)\,\Phi_n(Q,q) \tag{3-7}$$

and

$$(\hat{T}_q + U_n(q))\Theta_{nv}(q) = E_{nv}\Theta_{nv}(q) \tag{3-8}$$

The basis sets will be limited only to harmonic approximation for the vibron system and phonon bath

$$\Phi_n(Q,q) = \prod_l X_{n_l}(Q_l) \qquad \Theta_{nv}(q) = \prod_j \chi_{nvj}(Q_j(n)) \tag{3-9}$$

and

$$U_n(q) = \sum_l\left(n_l + \frac{1}{2}\right)\hbar\omega_l + \frac{1}{2}\sum_j\{\omega_j(n)\}^2\{q_j(n)\}^2 -$$
$$\sum_j \frac{1}{2\{\omega_j(n)\}^2}\left(\sum_l V_{llj}\left(v_l + \frac{1}{2}\right)\frac{\hbar}{\omega_l}\right)^2 + \hat{H}'' \tag{3-10}$$

where

$$\{\omega_j(n)\}^2 = \omega_j^2 + 2\sum_l V_{lljj}\left(v_l + \frac{1}{2}\right)\frac{\hbar}{\omega_l} \tag{3-11}$$

$$\{q_j(n)\}^2 = q_j^2 + \frac{1}{\omega_j^2}\sum_l V_{llj}\left(n_l + \frac{1}{2}\right)\frac{\hbar}{\omega_l} \tag{3-12}$$

$$\hat{H}'' = \sum_l\sum_{j\neq k} V_{ljk}Q_l q_j q_k + \sum_{l\neq l'}\sum_j V_{ll'j}Q_l Q_{l'}q_j +$$
$$\sum_{l,l',l''} V_{ll'l''}Q_l Q_{l'}Q_{l''} + \sum_l\sum_{i,j,k} V_{lijk}Q_l q_i q_j q_k +$$
$$\sum_l\sum_{j\neq k} V_{lljk}Q_l^2 q_j q_k + \sum_{l\neq l'}\sum_{j,k} V_{ll'jk}Q_l Q_{l'}q_j q_k + \cdots \tag{3-13}$$

and

$$E_{nv} = \sum_l\left(n_l + \frac{1}{2}\right)\hbar\omega_l + \sum_j\left(v_j + \frac{1}{2}\right)\hbar\omega_j(n) -$$
$$\sum_j \frac{1}{2\{\omega_j(n)\}^2}\left[\sum_l V_{llj}\left(v_l + \frac{1}{2}\right)\frac{\hbar}{\omega_l}\right] \tag{3-14}$$

Here, we use the following notations, for example,

$$V_{ljk} = \frac{1}{3!}\left(\frac{\partial^3 V}{\partial Q_l \partial q_j \partial q_k}\right)_0 \tag{3-15}$$

3.1. Intermolecular Vibrational Energy Transfer. We first consider the vibrational energy transfer between two molecules

D and A. In the dipole−dipole interaction[15]

$$\hat{H}'_{\text{VET}} = \frac{1}{4\pi\epsilon\epsilon_0 R_{\text{DA}}^3}\left[(\vec{\mu}_{\text{D}}^l\cdot\vec{\mu}_{\text{A}}^{l'}) - \frac{3(\vec{\mu}_{\text{D}}^l\cdot\vec{R}_{\text{DA}})(\vec{\mu}_{\text{A}}^{l'}\cdot\vec{R}_{\text{DA}})}{R_{\text{DA}}^2}\right] =$$
$$\frac{|\vec{\mu}_{\text{D}}^l||\vec{\mu}_{\text{A}}^{l'}|}{4\pi\epsilon\epsilon_0 R_{\text{DA}}^3}\Omega_{\text{DA}} \tag{3-16}$$

where ϵ and ϵ_0 denote the dielectric constant of the media and the permittivity of a vacuum, respectively, and R_{DA} represents the distance between the donor and acceptor molecules. Here $\vec{\mu}_{\text{D}}^l$ and $\vec{\mu}_{\text{A}}^{l'}$ are given by

$$\vec{\mu}_{\text{D}}^l = \left(\frac{\partial\vec{\mu}}{\partial Q_l}\right)Q_l \qquad \vec{\mu}_{\text{A}}^{l'} = \left(\frac{\partial\vec{\mu}'}{\partial Q_{l'}}\right)Q_{l'} \tag{3-17}$$

Using the Fermi Golden rule

$$W_{\text{VET}} = \frac{2\pi}{\hbar}\sum_v\sum_{v'}\rho_{nv}^{(b)}|\langle nv|\hat{H}'_{\text{VET}}|n'v'\rangle|^2 D(E_{n'v'} - E_{nv}) \tag{3-18}$$

for $(n_{\text{D}}^l = 1, n_{\text{A}}^{l'} = 0) \rightarrow (n_{\text{D}}^l = 0, n_{\text{A}}^{l'} = 1)$, we obtain

$$W_{\text{VET}} = \frac{2\pi}{\hbar^2}\frac{1}{(4\pi\epsilon\epsilon_0)^2 R_{\text{DA}}^6}\left|\left(\frac{\partial\vec{\mu}}{\partial Q_l}\right)_0\right|^2\left|\left(\frac{\partial\vec{\mu}'}{\partial Q_{l'}}\right)_0\right|^2|\Omega_{\text{DA}}|^2\left(\frac{1}{4\beta_l\beta_{l'}}\right) \times$$
$$\sum_v\sum_{v'}\rho_{nv}^{(b)}|\langle\Theta_{nv}|\Theta_{n'v'}\rangle|^2 D(\omega_{l'} - \omega_l - \omega_{v'v}) \tag{3-19}$$

The simplest case will be resonance energy transfer, i.e., $\omega_l = \omega_{l'}$, that is, the vibrational energy transfer of the same vibrational mode between two molecules. In this case, eq 3-19 reduces to

$$W_{\text{VET}} =$$
$$\frac{2\pi}{\hbar^2}\frac{1}{(4\pi\epsilon\epsilon_0)^2 R_{\text{DA}}^6}\left|\left(\frac{\partial\vec{\mu}}{\partial Q_l}\right)_0\right|^2\left|\left(\frac{\partial\vec{\mu}'}{\partial Q_{l'}}\right)_0\right|^2|\Omega_{\text{DA}}|^2\left(\frac{1}{4\beta_l\beta_{l'}}\right) \times$$
$$D(\omega_{l'} - \omega_l) \tag{3-20}$$

where Ω_{DA} describes the relative orientation between D and A, and

$$D(\omega_{l'} - \omega_l) = \frac{1}{\pi}\frac{\gamma_{10}}{\gamma_{10}^2 + (\omega_{l'} - \omega_l)^2} \tag{3-21}$$

Here γ_{10} denotes the dephasing rate constant associated with the population decay and the pure dephasing. As in the electronic energy transfer case, the vibrational energy transfer rate can be expressed in terms of spectral overlap. This can be accomplished as follows. For simplicity, we replace the Lorenzian $D(\omega_{l'} - \omega_l + \omega_{v'v})$ by the delta function $\delta(\omega_{l'} - \omega_l + \omega_{v'v})$

$$\delta(\omega_{l'} - \omega_l + \omega_{v'v}) =$$
$$\int d\omega\,[\delta(\omega_l + \omega_{v'v} - \omega)]_{\text{D}}[\delta(\omega + \omega_{v'v} - \omega_{l'})]_{\text{A}} \tag{3-22}$$

and assume that $|\langle\Theta_{nv}|\Theta_{n'v'}\rangle|^2 = |\langle\Theta_{nv}|\Theta_{n'v'}\rangle|^2_{\text{D}}|\langle\Theta_{nv}|\Theta_{n'v'}\rangle|^2_{\text{A}}$ and $\rho_{nv}^{(b)} = [\rho_{nv}^{(b)}]_{\text{D}}[\rho_{nv}^{(b)}]_{\text{A}}$. Then we can rewrite eq 3-19 as

$$W_{\text{VET}} = \frac{2\pi}{\hbar^2}\frac{1}{(4\pi\epsilon\epsilon_0)^2 R_{\text{DA}}^6}\left|\left(\frac{\partial\vec{\mu}}{\partial Q_l}\right)_0\right|^2\left|\left(\frac{\partial\vec{\mu}'}{\partial Q_{l'}}\right)_0\right|^2|\Omega_{\text{DA}}|^2\left(\frac{1}{4\beta_l\beta_{l'}}\right) \times$$
$$\int d\omega\left[\sum_v\sum_{v'}\rho_{nv}^{(b)}|\langle\Theta_{nv}|\Theta_{n'v'}\rangle|^2\delta(\omega_l + \omega_{v'v} - \omega)\right]_{\text{D}} \times$$
$$\left[\sum_v\sum_{v'}\rho_{nv}^{(b)}|\langle\Theta_{nv}|\Theta_{n'v'}\rangle|^2\delta(\omega + \omega_{v'v} - \omega_{l'})\right]_{\text{A}} \tag{3-23}$$

Time-Resolved SFG of Vibrational Dynamics of Water

J. Phys. Chem. A, Vol. 111, No. 37, 2007 **9065**

which should be compared with the band-shape function

$$\alpha(\omega) = \frac{4\pi^2\omega}{3\hbar c}\left|\left(\frac{\partial\bar{\mu}}{\partial Q_l}\right)_0\right|^2\left(\frac{1}{2\beta_l}\right)\sum_v\sum_{v'}\rho_{nv}^{(b)}|\langle\Theta_{nv}|\Theta_{n'v'}\rangle|^2 \times$$
$$\delta(\omega_{n'v',nv} - \omega) \quad (3\text{-}24)$$

3.2. One-Vibron Relaxation. In this case, the vibrational relaxation can be described by $n_l = 1 \rightarrow n_l = 0$; that is, the excitation energy of a vibron is directly relaxed into the phonon bath. Using the $\hat{H}''$ given by

$$\hat{H}'' = \sum_l\sum_{j\neq k}V_{ljk}Q_lq_jq_k \quad (3\text{-}25)$$

we obtain

$$W_{VET} = \frac{2\pi}{\hbar^2}\sum_{j,k}|V_{ljk}|^2\frac{(\bar{v}_j+1)(\bar{v}_k+1)}{8\beta_l\beta_j\beta_k} \times$$
$$\sum_{\{v_m\}}\sum_{\{v'_m\}}\prod_m^{m\neq j,k}\rho_{v_m}^{(b)}|\langle\chi_{v'_m}|\chi_{v_m}\rangle|^2D(-\omega_l+\omega_j+\omega_k+\omega_{v'v}) \quad (3\text{-}26)$$

or

$$W_{VET} = \frac{1}{\hbar^2}\sum_{j,k}|V_{ljk}|^2\frac{(\bar{v}_j+1)(\bar{v}_k+1)}{8\beta_l\beta_j\beta_k}\int_{-\infty}^{\infty}dt \times$$
$$\exp[it(-\omega_l+\omega_j+\omega_k)-\gamma_{10}|t|] \times$$
$$\exp\left\{\sum_m^{m\neq j,k}S_m[-(2\bar{n}_m+1)+(\bar{n}_m+1)e^{it\omega_m}+\bar{n}_me^{-it\omega_m}]\right\} \quad (3\text{-}27)$$

This represents the case in which the one quantum excitation energy of the vibron mode Q_l relaxes into the phonon modes q_j and q_k with one quantum each and the rest of all phonon modes whose the energy matches $\Delta = \hbar\omega_j + \hbar\omega_k - \hbar\omega_l$. Here the summations can be replaced by an integral with the density of state $\rho(E_j)$

$$\sum_j \rightarrow \int dE_j\,\rho(E_j) \quad (3\text{-}28)$$

3.3. Two-Vibron Relaxation. Next we consider the case of relaxation $(n_l = 1, n_{l'} = 0) \rightarrow (n_l = 0, n_{l'} = 1)$. In this case, we can use

$$\hat{H}'' = \sum_j V_{ll'j}Q_lQ_{l'}q_j \quad (3\text{-}29)$$

to obtain the rate of vibrational relaxation as

$$W_{VET} = \frac{2\pi}{\hbar^2}\sum_j|V_{ll'j}|^2\frac{(\bar{v}_j+1)}{8\beta_l\beta_{l'}\beta_j} \times$$
$$\sum_{\{v_m\}}\sum_{\{v'_m\}}\prod_m^{m\neq j}\rho_{vm}^{(b)}|\langle\chi_{v'_m}|\chi_{v_m}\rangle|^2D(\omega_{l'}-\omega_l+\omega_j+\omega_{v'v}) \quad (3\text{-}30)$$

or

$$W_{VET} = \frac{1}{\hbar^2}\sum_j|V_{ll'j}|^2\frac{(\bar{v}_j+1)}{8\beta_l\beta_{l'}\beta_j}\int_{-\infty}^{\infty}dt \times$$
$$\exp[it(\omega_{l'}-\omega_l+\omega_j)-\gamma_{10}|t|] \times$$
$$\exp\left\{\sum_m^{m\neq j}S_m[-(2\bar{n}_m+1)+(\bar{n}_m+1)e^{it\omega_m}+\bar{n}_me^{-it\omega_m}]\right\} \quad (3\text{-}31)$$

TABLE 1: Optimized Geometry of Single Water Molecule

atom	x^a	y^a	z^a
O	0.000000	0.000000	0.117041
H	0.000000	0.763487	−0.468165
H	0.000000	−0.763487	−0.468165

^{a} Unit of Å.

3.4. Three-Vibron Relaxation. This corresponds to the process $(n_1 = 1, n_{l'} = 0) \rightarrow (n_l = 0, n_{l'} = 2)$. Using

$$\hat{H}'' = V_{ll'r'}Q_lQ_{l'}^2 \quad (3\text{-}32)$$

we obtain

$$W_{VET} = \frac{1}{\hbar^2}|V_{ll'r'}|^2\frac{1}{4\beta_l\beta_{l'}^2} \times$$
$$\sum_v\sum_{v'}\rho_v^{(b)}|\langle\Theta_{n'v'}|\Theta_{nv}\rangle|^2D(2\omega_{l'}-\omega_l+\omega_{n'v',nv}) \quad (3\text{-}33)$$

or

$$W_{VET} = \frac{1}{\hbar^2}|V_{ll'r'}|^2\frac{1}{4\beta_l\beta_{l'}^2}\int_{-\infty}^{\infty}dt\,\exp[it(2\omega_{l'}-\omega_l)-\gamma_{10}|t|] \times$$
$$\exp\left\{\sum_j S_j[-(2\bar{n}_j+1)+(\bar{n}_j+1)e^{it\omega_j}+\bar{n}_je^{-it\omega_j}]\right\} \quad (3\text{-}34)$$

It should be noted that eq 3-33 can also be expressed in terms of spectral overlap.

Another possibility will be due to

$$\hat{H}'' = \sum_j V_{ll'r'j}Q_lQ_{l'}^2q_j \quad (3\text{-}35)$$

This case can be treated similarly and will not be discussed here.

3.5. Vibrational Spectroscopy. The quantum mechanical expression for the absorption coefficient of vibrational spectra has been given by eq 3-24. Notice that

$$|\langle\Theta_{nv}|\Theta_{n'v'}\rangle|^2 = \prod_i|\langle\chi_{nv_i}|\chi_{n'v'_i}\rangle|^2 \quad (3\text{-}36)$$

and that the spectral band-shape function can be expressed as

$$\alpha(\omega) = \frac{2\pi\omega}{3\hbar c}\left|\left(\frac{\partial\bar{\mu}}{\partial Q_l}\right)_0\right|^2\left(\frac{1}{2\beta_l}\right)\int_{-\infty}^{\infty}dt \times$$
$$\exp[it(\omega_{n'n}-\omega)-\gamma_{n'n}|t|]\prod_i G_i(t) \quad (3\text{-}37)$$

where

$$G_i(t) = \exp[S_i\{-(2\bar{n}_i+1)+(\bar{n}_i+1)e^{it\omega_i}+\bar{n}_ie^{-it\omega_i}\}] \quad (3\text{-}38)$$

where $\bar{n}_i$ denotes the phonon distribution function.

To show an application, we shall consider the theoretical treatments of sidebands in vibrational spectroscopy. A typical sideband in water can be described by $(n_l = 0, v_j = 0) \rightarrow (n_l = 1, v_j = 1)$, that is a combination band;[16,17] its transition moment is given by $\langle(n_l = 0, v_j = 0)|(\partial\bar{\mu}/\partial Q_l)_0Q_l|(n_l = 1, v_j = 1)\rangle$. Conventionally, it can be treated as follows. Due to the anharmonic coupling, the state $(n_l = 0, v_j = 0)$ can couple with the state $(n_l = 0, v_j = 1)$, and the state $(n_l = 1, v_j = 1)$ can

couple with ($n_l = 0$, $v_j = 1$). We find

$$\langle (n_l = 0, v_j = 0)|\left(\frac{\partial \vec{\mu}}{\partial Q_l}\right)_0 Q_l|(n_l = 1, v_j = 1)\rangle =$$

$$\frac{\langle (n_l = 0, v_j = 0)|V_{llj}Q_l^2 q_j|(n_l = 0, v_j = 1)\rangle}{-\hbar \omega_j} \times$$

$$\langle (n_l = 0, v_j = 1)|\left(\frac{\partial \vec{\mu}}{\partial Q_l}\right)_0 Q_l|(n_l = 1, v_j = 1)\rangle +$$

$$\frac{\langle (n_l = 1, v_j = 0)|V_{llj}Q_l^2 q_j|(n_l = 1, v_j = 1)\rangle}{\hbar \omega_j} \times$$

$$\langle (n_l = 0, v_j = 0)|\left(\frac{\partial \vec{\mu}}{\partial Q_l}\right)_0 Q_l|(n_l = 1, v_j = 0)\rangle =$$

$$\left(\frac{\partial \vec{\mu}}{\partial Q_l}\right)_0 \frac{V_{llj}}{\hbar \omega_j} \sqrt{\frac{1}{4\beta_j \beta_l}} \quad (3\text{-}39)$$

The transition moment for the fundamental transition is given by

$$\langle (n_l = 0, v_j = 0)|\left(\frac{\partial \vec{\mu}}{\partial Q_l}\right)_0 Q_l|(n_l = 1, v_j = 0)\rangle = \left(\frac{\partial \vec{\mu}}{\partial Q_l}\right)_0 \sqrt{\frac{1}{2\beta_l}}$$
$$(3\text{-}40)$$

The intensity ratio between these two bands is given by

$$R = \frac{\hbar |V_{llj}|^2}{2\omega_j^3 \omega_l^3} \quad (3\text{-}41)$$

In liquid water, a sideband at 2150 cm^{-1} has been observed and it has been attributed to $\delta_{OH} + \gamma_L$ where δ_{OH}(bending) = 1640 cm^{-1} and γ_L(librational mode) = 505 cm^{-1}. From the above discussion we can estimate the relative band-intensity of this sideband to the δ_{OH} band.

Another well-known sideband is observed at 2530 cm^{-1}, which has been attributed to $\delta_{OH} - \gamma_L$, where δ_{OH} = 3250 cm^{-1} and γ_L = 720 cm^{-1}. This sideband is a hot band and the vibrational transition can be described by ($v_{OH} = 0$, $v_L = 1$) → ($v_{OH} = 1$, $v_L = 0$). From eq 3-24 we can see that this band can be described by $\rho_{n,v_L=1}|\langle \Phi_{n'=1}|Q_l|\Phi_{n=0}\rangle|^2 |\langle \Theta_{n'=1,v'=0}|\Theta_{n=0,v=1}\rangle|^2$. Due to $\rho_{n=0,v=1}$, this sideband intensity will be weaker compared with the type discussed in the previous paragraph.

Similar to the electronic spectroscopy, $|\langle \Theta_{n'v'}|\Theta_{nv}\rangle|^2$ in eq 3-27 denotes the Franck−Condon factor. For example, for the transition ($n_l = 0$, $v_j = 0$) → ($n_l = 1$, $v_j = 1$), the intensity ratio between this transition and the transition ($n_l = 0$, $v_j = 0$) → ($n_l = 1$, $v_j = 0$) is given by

$$R = \frac{|\langle \chi_{1,1_j}|\chi_{0,0_j}\rangle|^2}{|\langle \chi_{1,0}|\chi_{0,0_j}\rangle|^2} \quad (3\text{-}42)$$

If we ignore the frequency change between the vibron states, i.e., the displaced oscillator case, R takes the form

$$R = S_j = \frac{\omega_j}{2\hbar} \Delta q_j(n)^2 \quad (3\text{-}43)$$

Using eq 3-12 for calculating $\Delta q_j(n)$ we can see that eq 3-43 reduces to eq 3-41. This shows that eq 3-24 can be used to calculate vibration spectra of molecules in dense media.

4. Discussion

Vibrational spectroscopic and dynamic properties require some of the fundamental properties of molecular systems, as

TABLE 2: Normal Modes and Transition Moment Derivative^a with Respect to Each Normal Mode

normal mode	frequency/cm^{-1}	$\partial \mu_x / \partial Q_i$	$\partial \mu_y / \partial Q_i$	$\partial \mu_z / \partial Q_i$
Q_1 (a1)	3819	9.2×10^{-10}	4.2×10^{-9}	-3.0
Q_2 (a1)	1602	7.0×10^{-10}	2.4×10^{-9}	-8.2
Q_3 (b2)	3924	-1.2×10^{-8}	-7.5	1.9×10^{-8}

^{a} Unit of $D/(\text{Å amu})^{1/2}$.

TABLE 3: Optimized Geometry of Dimer

atom	eq no.	x^a	y^a	z^a
O	1	-0.006242	1.525404	0.000000
H	1a	0.909757	1.525404	0.000000
H	1b	0.035907	0.556437	0.000000
O	2	-0.006242	-1.376356	0.000000
H	2a	-0.422895	-1.782687	0.767083
H	2b	-0.422895	-1.782687	-0.767083

^{a} Unit of Å.

TABLE 4: Unit Vectors^a of Dipole Moment Derivatives Originated at Each O Atom

O no.	$\hat{e}_x$	$\hat{e}_y$	$\hat{e}_z$
1	0.81977	-0.572693	0.000000
2	-0.715913	-0.698177	0.004215

^{a} $\hat{e}_n = (\partial \vec{\mu}_n / \partial Q_l)/[(\partial \vec{\mu}/\partial Q_l) \cdot (\partial \vec{\mu}/\partial Q_l)]^{1/2}$, where n specifies the oxygen atom.

shown in the previous sections. For example, normal modes, dipole moment derivatives, and anharmonic couplings are needed to estimate rate constants or model spectroscopic features. Quantum chemistry approaches could provide these properties: however, it is practically impossible to treat a whole water system. Here we shall treat water clusters and obtain vibrational properties and anharmonic couplings of water clusters (H$_2$O)$_n$ with n = 1, 2, ..., 8. We perform quantum chemistry calculations by using Gaussian 03[18] DFT at the B3LYP level and with the 6-311++G** basis set.
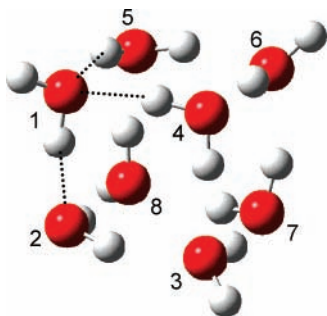
Next we shall estimate the rate of intermolecular energy transfer. The transfer rate for the resonance case can be expressed as (see eq 3-18)

$$W = \frac{2\pi}{\hbar^2}|H'_{DA}|^2 \frac{1}{\pi} \frac{\gamma_{DA}}{(\gamma_{DA})^2 + (\Delta \omega)^2} \quad (4\text{-}1)$$

where the coupling is given by

$$H'_{DA} = \frac{1}{4\pi \epsilon \epsilon_0 R_{DA}^3} \left[(\vec{\mu}_D^l \cdot \vec{\mu}_A^{l'}) - \frac{3(\vec{\mu}_D^l \cdot \vec{R}_{DA})(\vec{\mu}_A^{l'} \cdot \vec{R}_{DA})}{R_{DA}^2} \right] \quad (4\text{-}2)$$

Let us first consider a dimer cluster. In this example, we assume a model system in which each water molecule has its own normal modes and they are coupled with each other via the interaction defined by eq 4-2. $\vec{\mu}_D^l$ in eq 4-2, for example, is defined by eq (3−17) so that we make use of the calculated geometry and dipole moment derivatives for the water monomer, and they are listed in Table 1 and Table 2. To estimate the magnitude of eq 4-2, we further use the vacuum permittivity 8.854×10^{-12} J^{-1} C^2 m^{-1}. The optimized structure of the dimer is given in Table 3, and the distance between the two oxygen atoms is separated by $R_{O-O} = R_{DA}$ = 2.901 76 Å. If we choose a bending mode of 1602 cm^{-1} and place its dipole moment derivatives on each oxygen atom with the direction given in Table 4, the corresponding orientation factor is then Ω_{DA} = $-1.386\,57$ and the estimated value for the interaction is given by $|H'_{DA}|/2\pi c\hbar$ = 3.549 71 cm^{-1}.

Time-Resolved SFG of Vibrational Dynamics of Water

J. Phys. Chem. A, Vol. 111, No. 37, 2007 **9067**

Figure 1. Structure of water cube octamer. The numbers correspond to the oxygen molecules listed in Table 5.
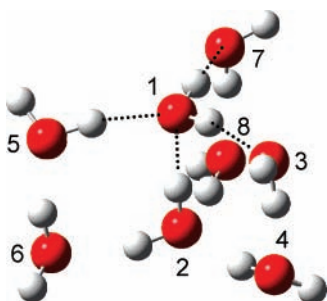
Figure 2. Structure of water bicyclic octamer. Each number specifies the oxygen molecule used in Figure 4.

Suppose that $\Delta\omega = 0$ in eq 4-1,

$$W = \frac{2}{\hbar^2}|H'_{DA}|^2 \frac{1}{\gamma_{DA}} \tag{4-3}$$

If the dephasing rate constant $\gamma_{DA} = 10^{12}$ s^{-1}, we find $W = 2|H'_{DA}/\hbar|^2(1/\gamma_{DA}) = 8\pi^2c^23.54971^2(1/10^{12}) \sim 8.954\,03 \times 10^{11}$ s^{-1} which is 1.116 82 ps.

Now we estimate the time constants for the intermolecular energy transfer in two octamers (cube and bicyclic) in a similar fashion. Figures 1 and 2 show the optimized structure of cube and bicyclic octamers, respectively, that agree with Ohno's work.[19] Table 5 lists the optimized molecular parameters for the cube octamer. For the cube case, the total number of possible two water molecule pair is 28. Table 6 lists the unit vectors of the dipole moment derivatives originated at each O atom. For the case in which $R_{O-O} < 3$ Å, we find that there are 12 water molecule pairs. Table 7 summarizes R_{O-O}, Ω, and the calculated rate constants, and these values versus H$_2$O pairs are plotted in Figure 3. Here the numbers 1−8 specify the oxygen atoms listed in Table 5. One can see from Figure 3 that there can be three groups for the energy transfer mechanism: the first group consisting of two water molecules with short distances around 2.68 Å and $|\Omega|$ values around 1.2, and the second group with longer distances around 2.86 Å and larger $|\Omega|$ around 1.38, the last group with similar distances as the second group and smaller $|\Omega|$ values $\sim$0.36. For the first group, the alignment of the two water molecules in each pair is similar to that of the dimer given in Table 1, and for the second group, the two water molecules form a tilted dimer structure, but this alignment is more preferable to have a larger value for$|\Omega|$. In the last group, the dimer structures are quite different from that listed in Table 1. We also estimate the intermolecular energy transfer time constants for molecular pairs whose R_{O-O} is larger than 3 Å. Table 8 lists the calculated time constants. The shortest time constant in this case is about 60 ps. The molecular pair in this group is located diagonally either in each plane in the cube (e.g., 1 ↔ 3 pair) or in the cube (e.g., 1 ↔ 7 pair).

TABLE 5: Optimized Geometry of the Cube Octamer

atom	eq no.	X^a	Y^a	Z^a
O	1	1.566303	1.449495	−1.285755
H	1a	1.642469	0.465981	−1.412737
H	1b	2.219554	1.861437	−1.859035
O	2	1.477277	−1.228116	−1.392212
H	2a	0.547244	−1.424396	−1.608627
H	2b	1.582434	−1.516535	−0.467514
O	3	−1.379417	−1.375764	−1.539816
H	3b	−1.515428	−1.502382	−0.562028
H	3b	−1.966234	−1.989406	−1.991442
O	4	−1.298728	1.485903	−1.308213
H	4a	−0.346812	1.643307	−1.445290
H	4b	−1.441147	0.568211	−1.602903
O	5	1.287805	1.214574	1.359794
H	5a	0.340021	1.421122	1.662674
H	5b	1.512659	1.500452	0.661773
O	6	−1.554271	1.386748	1.359794
H	6a	−1.571839	1.521934	0.375568
H	6b	−2.180900	2.006591	1.744949
O	7	−1.468370	−1.47477	1.132528
H	7a	−1.647155	−0.557323	1.406315
H	7b	−0.544209	−1.636833	1.39733
O	8	1.366881	−1.458804	1.467499
H	8a	1.944994	−1.880499	2.110213
H	8b	1.444504	−0.475781	1.599667

^{a} Unit of Å.

TABLE 6: Unit Vectors^a of Dipole Moment Derivatives Originated at Each O Atom in the Cube Octamer

O no.	$\hat{e}_x$	$\hat{e}_y$	$\hat{e}_z$
1	0.636658	−0.472214	−0.609656
2	−0.706978	−0.405819	0.579217
3	−0.629753	−0.645315	0.432411
4	0.679273	−0.638178	−0.362378
5	−0.587233	0.415327	−0.694738
6	−0.565406	0.659135	−0.495839
7	0.644368	0.61664	0.452266
8	0.572913	0.463705	0.675832

^{a} $\hat{e}_n = (\partial\vec{\mu}_n/\partial Q)/[(\partial\vec{\mu}_n/\partial Q)\cdot(\partial\vec{\mu}_n/\partial Q)]^{-1/2}$ where n specifies the oxygen atom.
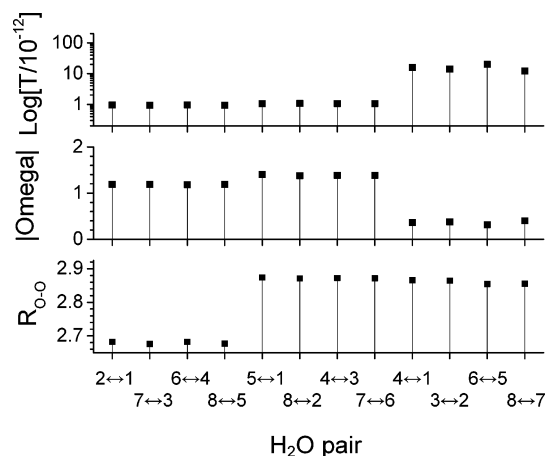
TABLE 7: Calculated Time Constants for the Intermolecular Energy Transfer in the Cube Octamer with $R_{O-O} < 3$ Å

	$R_{DA} = R_{O-O}{}^a$	Ω^b	$T = 1/(W \times 10^{-12})^c$
2 ↔ 1	2.68120	−1.18936	0.944596
4 ↔ 1	2.86535	−0.354928	15.8008
5 ↔ 1	2.87400	−1.40118	1.03235
3 ↔ 2	2.86431	−0.377116	13.9658
8 ↔ 2	2.87112	−1.37431	1.06669
4 ↔ 3	2.87216	−1.38538	1.05197
7 ↔ 3	2.67566	−1.19086	0.930579
6 ↔ 4	2.68205	−1.18375	0.955373
6 ↔ 5	2.85468	−0.312932	19.8762
8 ↔ 5	2.67633	−1.18819	0.936167
7 ↔ 6	2.87181	−1.38303	1.05479
8 ↔ 7	2.85501	−0.398997	12.235

^{a} Unit of Å. ^{b} Calculated using eq 4-2. ^{c} Calculated using eq 4-3 and unit of ps.

For the bicyclic octamer case, the time constants for the intermolecular energy transfer taking place in pairs with $R_{O-O} < 3$ Å are also calculated and shown in Figure 4. In this case, the time constants for the intermolecular energy transfer show strong $|\Omega|$ dependence.

It may be informative to estimate the time constants of the intermolecular energy transfer in the tetrahedral water cluster whose structure is shown in Figure 5. The calculated values are also plotted versus the water pair. If we look at the water

9068 *J. Phys. Chem. A, Vol. 111, No. 37, 2007*

Hayashi et al.

Figure 3. Calculated time constants for the intermolecular energy transfer in the cube octamer with $R_{O-O} < 3$ Å.

TABLE 8: Calculated VET Time Constants for the Intermolecular Energy Transfer in the Cube Octamer with $R_{O-O} > 3$ Å

|	$R_{DA} = R_{O-O}^{a}$	Ω^{b}	$T = 1/(W \times 10^{-12})^{c}$
3 ↔ 1	4.08949	−0.112493	1329.4
4 ↔ 2	3.88319	−0.105825	1506.79
5 ↔ 2	3.84032	−0.842586	66.6621
5 ↔ 3	4.84398	−0.234159	272.646
5 ↔ 4	3.87550	0.229208	234.729
6 ↔ 1	4.09156	0.00584479	337725.
6 ↔ 2	4.85812	−0.86013	63.9108
6 ↔ 3	4.00871	0.213419	272.517
7 ↔ 1	4.85887	−0.878554	60.1967
7 ↔ 2	3.88741	−0.24601	246.614
7 ↔ 4	3.84078	−0.125602	1041.53
7 ↔ 5	3.87507	0.231926	226.547
8 ↔ 1	4.00979	0.0306694	12274.4
8 ↔ 3	4.07345	−0.8504	64.3896
8 ↔ 4	4.84576	0.145168	577.869
8 ↔ 6	4.07945	−0.0778607	2734.42

a Unit of Å. *b* Calculated using eq 4-2. *c* Calculated using eq 4-3 and unit of ps.
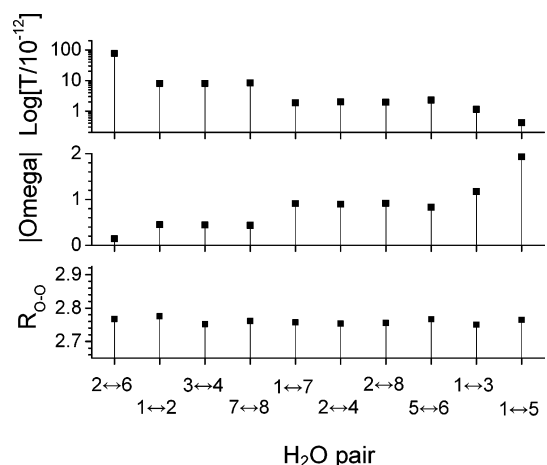
Figure 4. Calculated time constants for the intermolecular energy transfer in the bicyclic octamer with $R_{O-O} < 3$ Å.

molecule 2, there are 4 water pairs that consist of the nearest neighbor water molecules. The respective calculated time constants are 1.26 ps for the 1 ↔ 2 pair, 15.2 ps for the 2 ↔ 5 pair, 27.3 ps for the 2 ↔ 4 pair, and 44.0 ps for the 2 ↔ 3 pair.

According to the coupled oscillator model presented in section 3, to treat VER we need to have the information of cubic and quartic anharmonic coupling constants. In our DFT calculations
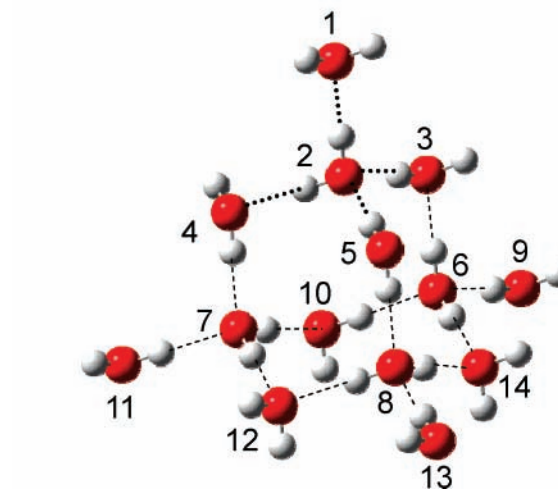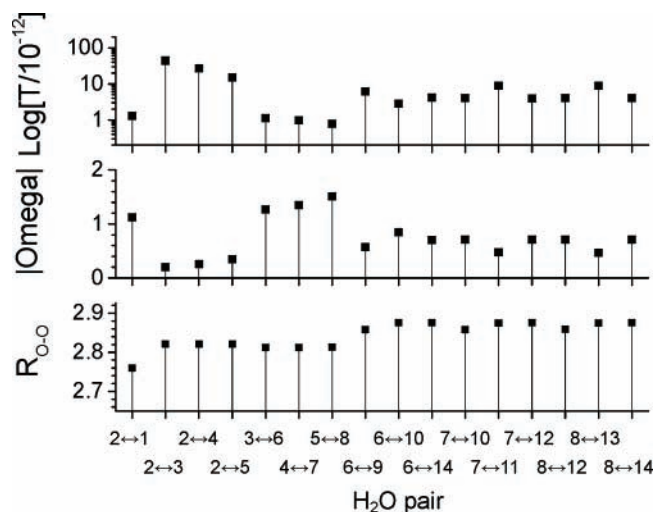
Figure 5. Structure and calculated time constants for the intermolecular energy transfer of the tetrahedral water cluster.

of water clusters, this information has been obtained up to the cluster of size 8. So, in principle, we should be able to perform the quantum chemistry calculations of the rates of energy transfer (see eqs 3-27, 3-31, and 3-34) and VER. For example, from Figure 1 for the cube octamer we can determine how the cluster is excited initially by the pumping laser (determined by laser wavelength, pulse duration, and laser intensity). Each excited state will evolve (or decay) and its dynamical process can be described by using the coupled oscillator model, which requires the information of cubic and quartic anharmonic couplings.

Two types of VER have been reported.[16,17] One is the VER of $\nu_{OH} = 3700$ cm^{-1} into two quanta of 1650 cm^{-1}. That is, this type of VER belongs to three-vibron processes $V_{ll'l'}Q_lQ_{l'}^{2}$. There are a number of possibilities (i.e., paths) found in our DFT calculations; the cubic anharmonic coupling constants cover the range 0−90 cm^{-1} (see Appendix S7 in the Supporting Information). Another type of VER is the so-called thermalization. In our opinion the most probable processes will be the VER of the 1650 cm^{-1} modes into two quanta of the vibrational modes with frequencies smaller than 1000 cm^{-1}. In this case, the cubic anharmonic coupling constants cover the range 0−102 cm^{-1} (see Appendix S7 in the Supporting Information). From the values of anharmonic coupling constants for VER in comparison with the $|H'_{DA}|$ values for vibrational energy transfer, the time scale of VER can also be estimated. In a future

Time-Resolved SFG of Vibrational Dynamics of Water

J. Phys. Chem. A, Vol. 111, No. 37, 2007 **9069**

paper, we shall report the detailed first-principle calculations of vibrational spectroscopy, VER, and vibrational energy transfer.

5. Conclusion

In this paper, using the density matrix method, we have developed a theory of time-resolved SFG that takes into account the dynamical behaviors of both population and coherence of the surface system. To study the vibrational dynamics of surface waters, we limit ourselves to discuss the case of time-resolved vibrational IR-UV SFG. To treat the VER, vibrational energy transfer, and vibrational spectroscopy of liquid water, we have used the coupled oscillator model in which the basis set chosen is based on the diabatic approximation to separate the system oscillators and bath oscillators. In the harmonic oscillator approximation, vibrational energy transfer, VER, and vibrational spectroscopy can be calculated by including cubic anharmonic couplings that are obtained by DFT calculations. In this way we have demonstrated that it is possible to carry out the first-principle calculations of vibrational spectroscopy and dynamics of clusters.

Supporting Information Available: The rectangular pulse treatments and derivation of pumping process are given in Appendices S1 and S2. A detailed derivation of $F_{gg}(T_{pump})$ and $F_{g'g'}(T_{pump})$ is presented in Appendix S3, that of $\sigma^{SFG}_{eg\leftarrow gg}(T_{SFG})$ and $\sigma^{SFG}_{g''e\leftarrow gg}(T_{SFG})$ is given in Appendix S4, and that of S_{12} and S_{22} is shown in Appendix S5, respectively. Appendix S6 shows a definition of $F_{g'g'}(T_{pump})$ and $F_{gg}(T_{pump})$. Normal modes and anharmonic coupling of cube octamer are given in Appendix S7. This material is available free of charge via the Internet at http://pubs.acs.org.

References and Notes

(1) McGuier, J. A.; Shen, Y. R. *Science* **2006**, *313*, 1945.
(2) Ishiyama, T.; Morita, A. *Chem. Phys. Lett.* **2006**, *78*, 431.
(3) Morita, A. *J. Phys. Chem. B* **2006**, *110*, 3158.
(4) Morita, A. *Chem. Phys. Lett.* **2004**, *398*, 361.
(5) Morita, A. *J. Phys. Chem. B* **2002**, *106*, 673.
(6) Morita, A. *Chem. Phys.* **2000**, 258.
(7) Hayashi, M.; Lin, S. H.; Shen, Y. R. *J. Phys. Chem. A* **2004**, *108*, 8058.
(8) Hayashi, M.; Lin, S. H.; Raschke, M. B.; Shen, Y. R. *J. Phys. Chem. A* **2002**, *106* 2271.
(9) Hayashi, M.; Lin, S. H. In *Advances in Multi-photon Processes and spectroscopy*; Lin, S. H., Fujimura, Y., Villaeys, A. A., Eds.; World Scientific: Singapore, 2004; Vol. 16, pp 307.
(10) Lin, S. H.; Hayashi, M.; Islampour, R.; Yu, J.; Yang, D. Y.; Wu, G. Y. C. *Physica B* **1996**, *222*, 191.
(11) Lin, S. H.; Alden, R.; Islampour, R.; Ma, H.; Villaeys, A. A. *Density Matrix Method and Femtosecond Processes*; World Scientific: Singapore, 1991; Chapter 1.
(12) Du, Q.; Superfine, R.; Freysz, E.; Shen, Y. R. *Phys. Rev. Lett.* **1993**, *70*, 2313.
(13) Shen, Y. R.; Ostroverkhov, V. *Chem. Rev.* **2006**, *106*, 1140.
(14) Lin, S. H. *J. Chem. Phys.* **1976**, *65*, 1053.
(15) Blumen, A.; Lin, S. H.; Mantz, J. *J. Chem. Phys.* **1978**, *69*, 881.
(16) Moskovits, M.; Michaelian, K. H. *J. Chem. Phys.* **1978**, *69*, 2306.
(17) Lock A. J.; Bakker, H. J. *J. Chem. Phys.* **2002**, *117*, 1708.
(18) Frisch, M. J.; Trucks, G. W.; Schlegel, H. B.; Scuseria, G. E.; Robb, M. A.; Cheeseman, J. R.; Montgomery, J. A., Jr.; Vreven, T.; Kudin, K. N.; Burant, J. C.; Millam, J. M.; Iyengar, S. S.; Tomasi, J.; Barone, V.; Mennucci, B.; Cossi, M.; Scalmani, G.; Rega, N.; Petersson, G. A.; Nakatsuji, H.; Hada, M.; Ehara, M.; Toyota, K.; Fukuda, R.; Hasegawa, J.; Ishida, M.; Nakajima, T.; Honda, Y.; Kitao, O.; Nakai, H.; Klene, M.; Li, X.; Knox, J. E.; Hratchian, H. P.; Cross, J. B.; Bakken, V.; Adamo, C.; Jaramillo, J.; Gomperts, R.; Stratmann, R. E.; Yazyev, O.; Austin, A. J.; Cammi, R.; Pomelli, C.; Ochterski, J. W.; Ayala, P. Y.; Morokuma, K.; Voth, G. A.; Salvador, P.; Dannenberg, J. J.; Zakrzewski, V. G.; Dapprich, S.; Daniels, A. D.; Strain, M. C.; Farkas, O.; Malick, D. K.; Rabuck, A. D.; Raghavachari, K.; Foresman, J. B.; Ortiz, J. V.; Cui, Q.; Baboul, A. G.; Clifford, S.; Cioslowski, J.; Stefanov, B. B.; Liu, G.; Liashenko, A.; Piskorz, P.; Komaromi, I.; Martin, R. L.; Fox, D. J.; Keith, T.; Al-Laham, M. A.; Peng, C. Y.; Nanayakkara, A.; Challacombe, M.; Gill, P. M. W.; Johnson, B.; Chen, W.; Wong, M. W.; Gonzalez, C.; Pople, J. A. *Gaussian 03*, revision C.02; Gaussian, Inc.: Wallingford, CT, 2004.
(19) Ohno, K.; Okimura, M.; Akaib, N.; Katsumotoa Y. *Phys. Chem. Chem. Phys.* **2005**, *7*, 3005.